Importance of the V $3d-O\ 2p$ hybridization in the Mott-Hubbard material V_2O_3

R. J. O. Mossanek and M. Abbate*
Departamento de Física, Universidade Federal do Paraná, Caixa Postal 19091, 81531-990 Curitiba PR, Brazil
(Received 7 December 2006; published 9 March 2007)

We studied the changes in the electronic structure of V_2O_3 using a cluster model. The calculations included fluctuations from the coherent band in the metallic phase and nonlocal Mott-Hubbard fluctuations in the insulating phase. The incoherent structure is mostly related to the usual ligand screening channel ($3d^2\underline{L}$). The coherent peak in the metallic phase corresponds to coherent band fluctuations ($3d^2\underline{C}$). However, The Mott-Hubbard screened state in the insulating phase ($3d^2\underline{D}$) appears at higher energies. The transfer of spectral weight from the $3d^2\underline{L}$ to the $3d^2\underline{D}$ state produces the opening of the band gap. The photon energy dependence of the spectra is partly related to the relative V $3d-O\ 2p$ cross sections. The calculations reproduce also the experimental changes observed in the V $1s$ core-level spectra. The above results suggest that the Mott-Hubbard transition in V_2O_3 requires a multiband model.

DOI: 10.1103/PhysRevB.75.115110 PACS number(s): 71.30.+h, 71.28.+d, 79.60.Bm

I. INTRODUCTION

Many early transition-metal oxides present a distinct metal-insulator transition (MIT).[1] The particularly interesting MIT in V_2O_3 can be triggered by temperature, pressure, or doping.[2] Pure V_2O_3 goes from an antiferromagnetic insulator phase below 150–170 K to a paramagnetic metal phase at higher temperatures.[3,4] The physics of this material is usually considered the paradigm of the Mott-Hubbard transition.

The first attempt to explain the MIT in V_2O_3 involved a mixed spin-orbital model.[5] The optical conductivity was investigated using the DMFT approach.[6] The electronic structure of V_2O_3 was calculated using the LDA+U and DMFT methods.[7,8] The orbital ordering was studied using RXS,[9,10] neutron scattering[11] and x-ray absorption spectroscopy[12] (XAS); these experimental results were explained in terms of spin coupling within the V-V pairs.[13]

The electronic structure of V_2O_3 was studied using photoemission spectroscopy[14,15] (PES) and XAS.[16] More recent attempts involved combined PES-XAS (Ref. 17) and XPS-XAS (Ref. 18) studies. The photoemission spectra of metallic V_2O_3 show a prominent quasiparticle peak;[19,20] the large intensity of this peak was attributed to larger bulk sensitivity at high photon energies. The satellite in the core-level spectra was attributed to screening from the coherent band.[21]

In this work, we studied the changes in the electronic structure of V_2O_3 using a cluster model. The calculation includes the screening from the coherent band in the metallic phase,[21,22] and a distinct Mott-Hubbard screening in the insulating phase.[23,24] A similar method was recently used to study the electronic structure of metallic and insulating VO_2.[25] The calculation reproduces the changes in the valence-band and the core-level spectra with temperature, as well as the changes in the metallic valence-band spectra as a function of the photon energy.

The above results suggest that the interpretation of the V_2O_3 PES spectra should be revised. The incoherent structure is usually attributed to the remnant of the lower Hubbard band.[6,8] The present calculation shows that it corresponds mostly to a ligand screened ($3d^2\underline{L}$) state. The photon energy dependence is usually ascribed to the relative surface to bulk contribution.[19,20] The results here suggest that the relative V $3d-O\ 2p$ cross section may also be an important factor.

Further, the standard DMFT approach does not include the O $2p$ states explicitly and thus cannot explain the observed charge-transfer satellites in the core-level spectra. On the other hand, the present method explains not only the charge-transfer satellites but also the lower binding energy satellites due to the screening from the coherent band. This suggests that the Mott-Hubbard transition in V_2O_3 requires a V $3d-O\ 2p$ multiband model.

II. CALCULATION DETAILS

The cluster considered here was composed by a V^{3+} ion surrounded by an O^{2-} octahedra. The cluster model was solved using the standard configuration-interaction method. The main parameters of the model are the charge-transfer energy Δ, the Mott-Hubbard energy U, the core-hole potential Q ($Q=1.25U$), and the p-d transfer integral T_σ.[26] The multiplet splitting was given in terms of the crystal field parameter $10Dq$ and the p-p transfer integral $pp\pi$-$pp\sigma$.

The metallic phase calculation includes the screening from the coherent band.[21,22] The screening charge, in this case, comes from a delocalized state at the Fermi level [Fig. 1(a)]. The metallic ground state was expanded in the $3d^2$,

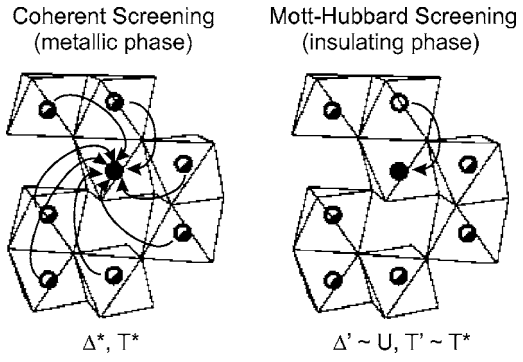

FIG. 1. Crystallographic structure and the nonlocal screening channels of metallic and insulating V_2O_3.

TABLE I. Configurations and energy levels of the metallic ground state.

Configuration	Energy level
$3d^2$	0
$3d^3\underline{C}$	Δ^*
$3d^3\underline{L}$	Δ
$3d^4\underline{C}^2$	$2\Delta^*+U$
$3d^4\underline{CL}$	$\Delta^*+\Delta+U$
$3d^4\underline{L}^2$	$2\Delta+U$

$3d^3\underline{C}$, $3d^3\underline{L}$, $3d^4\underline{C}^2$, $3d^4\underline{CL}$, $3d^4\underline{L}^2$, etc., configurations, where $\underline{C}$ denotes a hole in the coherent band and $\underline{L}$ designates a hole in the O $2p$ band. The additional parameters are the coherent charge-transfer energy Δ^* and the transfer integral T^*. The value of Δ^* corresponds roughly to the half-width of the occupied V $3d$ band, whereas T^* is related to the second-order intercluster hopping processes [Fig. 1(a)]. The configurations and energy levels of the metallic ground state are listed in Table I.

The calculation in the insulating phase included a typical Mott-Hubbard charge fluctuation. The screening charge, in this phase, comes from a single nearest-neighbor V^{3+} ion.[23,24] The insulating ground state was expanded in the $3d^2$, $3d^3\underline{D}$, $3d^3\underline{L}$, $3d^4\underline{D}^2$, $3d^4\underline{DL}$, $3d^4\underline{L}^2$, etc., configurations, were $\underline{D}$ denotes a hole in the neighboring V^{3+} site. The Mott-Hubbard fluctuation energy is $\Delta'=U$, and the intercluster transfer was set to $T'=T^*$ (because the lattice distortion in the insulating phase is small, and it does not affect intercluster hopping). The configurations and energy levels of the insulating ground state are listed in Table II.

The removal (core-level) state was obtained by removing a valence (core-level) electron from the ground state. Finally, the corresponding spectral weight was calculated using the sudden approximation.[26]

The model parameters used in the present calculation are listed in Table III. These values gave the best agreement with the experiment and are also in excellent agreement with previous estimates.[21,27] The transfer integrals T_σ and T^* were increased by 10% in the core-level calculations.

III. RESULTS AND DISCUSSION

The main compositions of the metallic and insulating V_2O_3 ground states are given in Table IV. The unscreened $3d^2$ configuration dominates the ground state in both phases,

TABLE II. Configurations and energy levels of the insulating ground state.

Configuration	Energy level
$3d^2$	0
$3d^3\underline{D}$	Δ'
$3d^3\underline{L}$	Δ
$3d^4\underline{D}^2$	$2\Delta'+U$
$3d^4\underline{DL}$	$\Delta'+\Delta+U$
$3d^4\underline{L}^2$	$2\Delta+U$

TABLE III. Parameters used in the cluster model calculations (all values in eV).

Parameter	Metallic V_2O_3	Insulating V_2O_3
Δ	5.0	
U	3.5	
T_σ	3.0	
$10Dq$	1.8	
$pp\pi$-$pp\sigma$	1.0	
Δ^*	0.90	
T^*	0.20	
Δ'		3.5 (U)
T'		0.20 (T^*)

but there is also a large O $2p$ contribution represented by the $3d^3\underline{L}$ configuration. Finally, the nonlocal screened configurations, $3d^3\underline{C}$ and $3d^3\underline{D}$, are much weaker. This is attributed to the relatively larger value of the local T_σ compared to the nonlocal T^* and T'.

Figure 2 shows the V $3d$ removal spectra of metallic and insulating V_2O_3. The corresponding spectra were decomposed in the main final configurations. In the metallic phase, the coherent peak, at about −0.3 eV, is mostly formed by the $3d^2\underline{C}$ configuration (40%), whereas the incoherent part, around −1.2 eV, is mainly formed by the $3d^2\underline{L}$ configuration (37%). There is also a lower energy state, around −7.4 eV, which is mostly formed by the $3d^1$ configuration (56%).

In the metallic removal state, the initial positions of the $3d^2\underline{C}$ and $3d^2\underline{L}$ configurations are determined by the Δ^* and Δ parameters, whereas the energy level of the $3d^1$ configuration is related to the value of U. The results show that both the coherent and incoherent structures are *well-screened* states. The screening charge in the coherent part comes from the coherent band ($3d^2\underline{C}$), whereas the screening fluctuations in the incoherent part come from the ligand ($3d^2\underline{L}$). On the other hand, the state around −7.4 eV corresponds to the *poorly screened* state ($3d^1$). The lowest energy fluctuation, in this phase, is from a $3d^2\underline{C}$ to a $3d^3$ configuration (d-d type). The material can be classified as a strongly V $3d$–O $2p$ hybridized Mott-Hubbard system.

In the insulating phase, the nonlocal screened configuration $3d^2\underline{C}$ is replaced by $3d^2\underline{D}$. The initial position of this configuration is now determined by the value of $\Delta'=U$. The corresponding peak about −3.3 eV ($\sim -U$) is given mostly by the $3d^2\underline{D}$ configuration (53%). The incoherent structure,

TABLE IV. Metallic and insulating V_2O_3 ground state decomposed in the main contributions.

Metallic V_2O_3		Insulating V_2O_3	
Configuration	Percent	Configuration	Percent
$3d^2$	52%	$3d^2$	53%
$3d^3\underline{C}$	2.5%	$3d^3\underline{D}$	1.5%
$3d^3\underline{L}$	38%	$3d^3\underline{L}$	40%

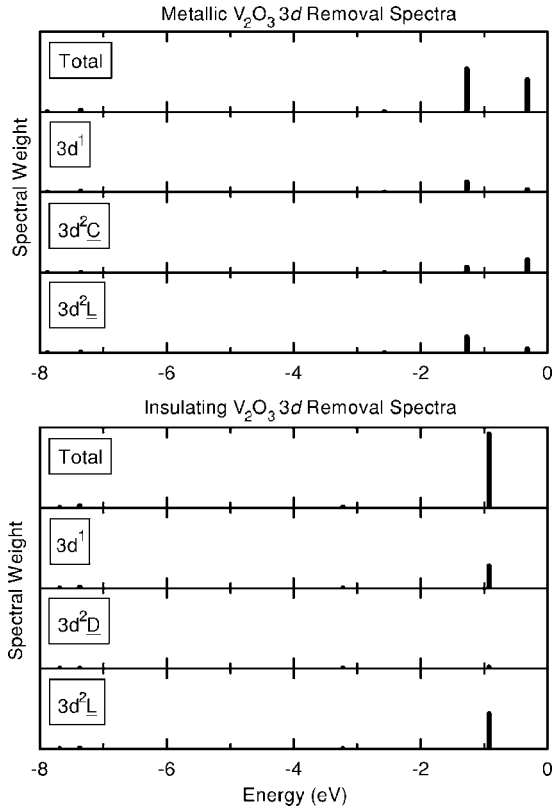

FIG. 2. V 3d removal spectra of metallic and insulating V_2O_3 projected on the main final-state configurations.

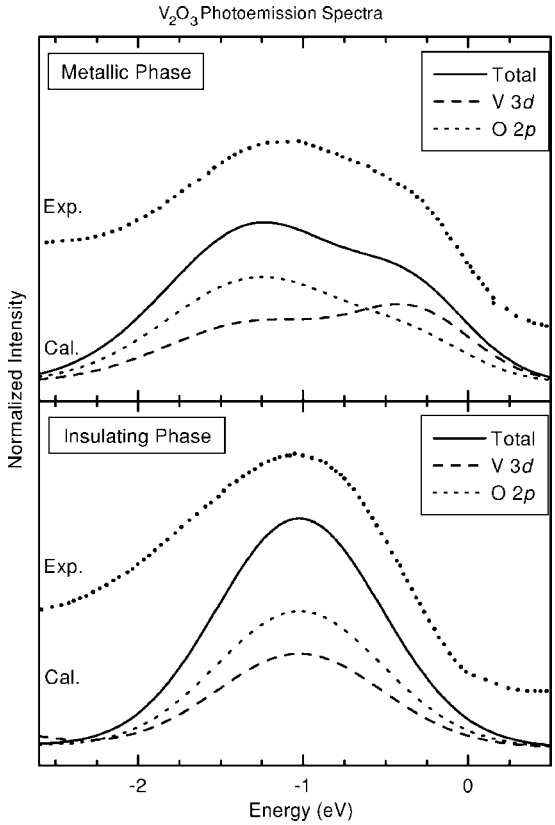

FIG. 3. Calculated removal spectra, decomposed into the V 3d and O 2p contributions, compared to the photoemission spectra taken from Ref. 17 ($h\nu$=50 eV).

around −1.1 eV, is still mainly formed by the $3d^2\underline{L}$ configuration (47%). Finally, the low-energy state, about −7.6 eV, is mostly formed by the $3d^1$ state (58%). The lowest energy fluctuation, in this case, is from a $3d^2\underline{L}$ to a $3d^3$ configuration (p-d type). This conclusion is supported by the positive value obtained for the Hall resistance R_H.[28]

The changes in the electronic structure are mostly related to the transfer of spectral weight. The coherent peak ($3d^2\underline{C}$) around $-\Delta^*$, in the metallic phase, is substituted by the Mott-Hubbard screened peak ($3d^2\underline{D}$) at about $-U$, in the insulating phase. This transfer of spectral weight produces the opening of the band gap in the insulating phase. The value of the band gap increases with the value of U, as it should be in the Mott-Hubbard regime.

The coherent structure, mostly $3d^2\underline{C}$, has an almost pure V 3d character, whereas the incoherent feature, mainly $3d^2\underline{L}$, is of mixed O 2p–V 3d character. In fact, the $3d^2\underline{C}$ final-state configuration can only be obtained by removing a V 3d electron from the $3d^3\underline{C}$ ground-state configuration, but the $3d^2\underline{L}$ final-state configuration can be reached by removing either a V 3d electron (from $3d^3\underline{L}$) or an O 2p electron (from $3d^2$).

Figure 3 shows the relative weight of the V 3d and O 2p contributions to the removal spectra, compared to photoemission spectra taken from Ref. 17. The discrete states were convoluted with a 0.5 eV Gaussian to simulate the resolution and band dispersion. The relative cross sections of the V 3d and O 2p levels were adjusted to a photon energy of 50 eV.[25] The calculation results are in excellent agreement with the experimental spectra and show that the incoherent structure contains considerable O 2p character.

Figure 4 shows the calculated removal states of metallic and insulating V_2O_3 compared to the valence-band photoemission spectra taken from Ref. 15. The O 2p contribution to the spectra was obtained using the independent particle approximation. The calculation is in relatively good agreement with the experimental results. The V 3d band in the metallic phase is formed by the $3d^2\underline{C}$ and $3d^2\underline{L}$ derived states, whereas in the insulating phase, the V 3d band region is attributed to the $3d^2\underline{L}$ derived state. The poorly screened $3d^1$ state appears at higher energies hidden in the O 2p band region. The existence of the $3d^1$ state is partially reflected in the resonant photoemission spectra of V_2O_3.[14,15]

Recent high-energy photoemission study of V_2O_3 showed a prominent coherent feature.[19,20] This enhancement is commonly attributed to the increased mean free path of the photon and the relatively larger bulk character of the coherent structure. On the other hand, the main contribution to the incoherent structure would come from the surface region. Figure 5 shows the calculated photoemission spectra at 60 and 700 eV, taking into account the relative V 3d and O 2p cross sections.[29] The calculated results show also a considerable increase of the coherent feature, which is similar to the behavior in the experimental spectra taken from Ref. 19. Thus, the present calculation suggests that the relatively V 3d/O 2p cross section should also be considered.

Figure 6 shows the calculated core-level spectra of V_2O_3 in both phases, compared to the V 1 s photoelectron spectra

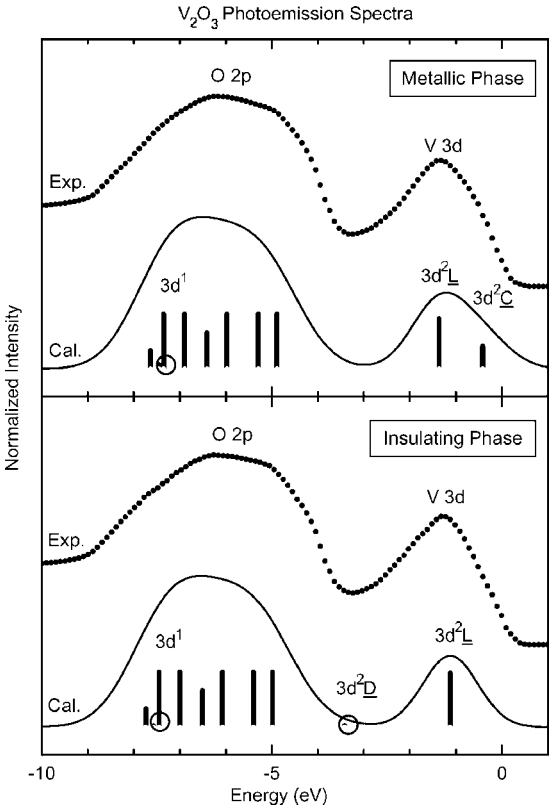

FIG. 4. Cluster model calculations of metallic and insulating V_2O_3 compared to the photoemission spectra taken from Ref. 15 ($h\nu$=60 eV).

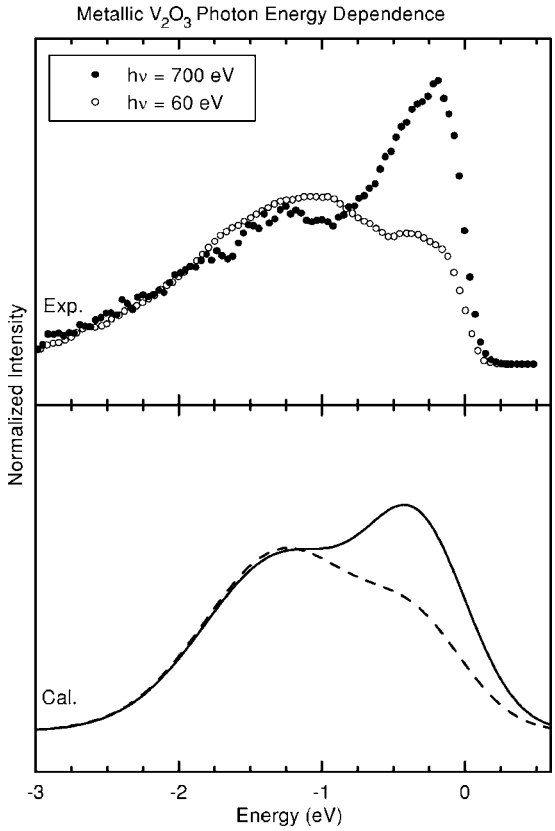

FIG. 5. Calculated photon energy dependence of the metallic spectra compared to the experimental spectra taken from Ref. 19 ($h\nu$=60–700 eV).

taken from Ref. 30. The discrete states were convoluted with a 1.0 eV Gaussian to simulate the experimental energy resolution. The main structure is dominated by the well-screened $c3d^3\underline{L}$ configuration, whereas the satellite peak is mostly formed by the poorly screened $c3d^2$ configuration. The low-energy shoulder in the metallic phase is mainly given by the nonlocal $c3d^3\underline{C}$ configuration and appears at lower energies because $\Delta^* < \Delta$. The nonlocal screened state in the insulating phase is formed mainly by the $c3d^3\underline{D}$ configuration and appears at higher energies because $\Delta' > \Delta$.

The calculated removal and core-level spectra present the same qualitative trends. Namely, they are formed by low-energy well-screened states ($3d^2\underline{L}$ or $c3d^3\underline{L}$) and high-energy poorly screened states ($3d^1$ or $c3d^2$). The lowest-energy states in the metallic phase are related to coherent fluctuations ($3d^2\underline{C}$ or $c3d^3\underline{C}$), which are replaced in the insulating phase by Mott-Hubbard screened states ($3d^2\underline{D}$ or $c3d^3\underline{D}$). However, differently from the removal state, the high-energy poorly screened state ($c3d^2$) appears clearly in the core-level spectra. The present model provides a consistent description of both the valence and core-level spectra, whereas a single-band model would be unable to explain the observed satellites in the core-level spectra.

IV. CONCLUSION

In conclusion, we studied the changes in the electronic structure of V_2O_3 using a cluster model. The changes in the

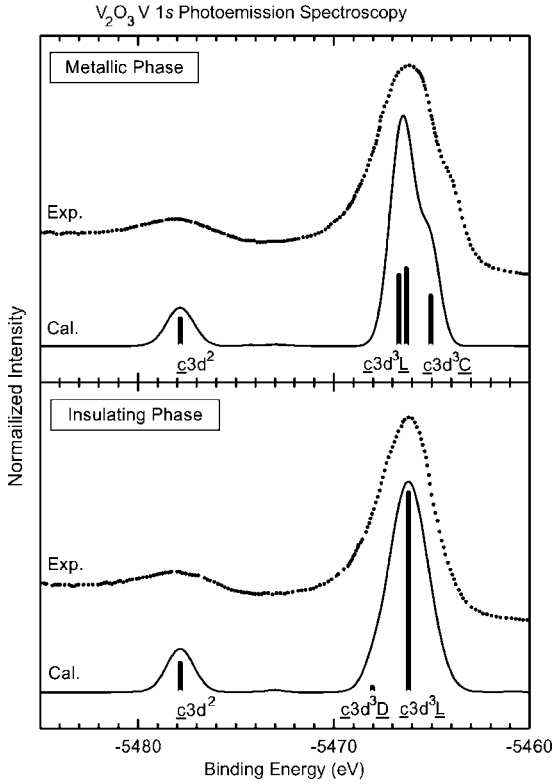

FIG. 6. Calculated V 1s core-level spectra compared to the experimental spectra taken from Ref. 30.

electronic structure can be related to the different nonlocal screening channels in each phase. In the metallic phase, the coherent state ($3d^2\underline{C}$) appears close to the Fermi level because Δ^* is relatively small. In the insulating phase, the Mott-Hubbard state ($3d^2\underline{D}$) appears at higher energies because $\Delta' = U$ is relatively large. The transfer of spectral weight from the $3d^2\underline{C}$ and $3d^2\underline{D}$ states produces the opening of the band gap. The results also indicate that the relative V $3d$/O $2p$ cross sections are partly responsible of the photon energy dependence. Finally, the present model reproduces the changes in both the valence-band and core-level spectra.

*Corresponding author. Electronic address: miguel@fisica.ufpr.br

[1] M. Imada, A. Fujimori, and Y. Tokura, Rev. Mod. Phys. **70**, 1039 (1998).
[2] D. B. McWhan, T. M. Rice, and J. P. Remeika, Phys. Rev. Lett. **23**, 1384 (1969); D. B. McWhan, A. Menth, J. P. Remeika, W. F. Brinkman, and T. M. Rice, Phys. Rev. B **7**, 1920 (1973).
[3] R. M. Moon, Phys. Rev. Lett. **25**, 527 (1970).
[4] J. B. Goodenough, Prog. Solid State Chem. **5**, 145 (1971).
[5] C. Castellani, C. R. Natoli, and J. Ranninger, Phys. Rev. B **18**, 4945 (1978).
[6] M. J. Rozenberg, G. Kotliar, H. Kajueter, G. A. Thomas, D. H. Rapkine, J. M. Honig, and P. Metcalf, Phys. Rev. Lett. **75**, 105 (1995); M. J. Rozenberg, G. Kotliar, and H. Kajueter, Phys. Rev. B **54**, 8452 (1996).
[7] S. Yu. Ezhov, V. I. Anisimov, D. I. Khomskii, and G. A. Sawatzky, Phys. Rev. Lett. **83**, 4136 (1999).
[8] K. Held, G. Keller, V. Eyert, D. Vollhardt, and V. I. Anisimov, Phys. Rev. Lett. **86**, 5345 (2001).
[9] M. Fabrizio, M. Altarelli, and M. Benfatto, Phys. Rev. Lett. **80**, 3400 (1998).
[10] L. Paolasini, C. Vettier, F. de Bergevin, F. Yakhou, D. Mannix, A. Stunault, W. Neubeck, M. Altarelli, M. Fabrizio, P. A. Metcalf, and J. M. Honig, Phys. Rev. Lett. **82**, 4719 (1999).
[11] W. Bao, C. Broholm, G. Aeppli, P. Dai, J. M. Honig, and P. Metcalf, Phys. Rev. Lett. **78**, 507 (1997); W. Bao, C. Broholm, G. Aeppli, S. A. Carter, P. Dai, T. F. Rosenbaum, J. M. Honig, P. Metcalf, and S. F. Trevino, Phys. Rev. B **58**, 12727 (1998).
[12] J.-H. Park, L. H. Tjeng, A. Tanaka, J. W. Allen, C. T. Chen, P. Metcalf, J. M. Honig, F. M. F. de Groot, and G. A. Sawatzky, Phys. Rev. B **61**, 11506 (2000).
[13] F. Mila, R. Shiina, F.-C. Zhang, A. Joshi, M. Ma, V. Anisimov, and T. M. Rice, Phys. Rev. Lett. **85**, 1714 (2000).
[14] K. E. Smith and V. E. Henrich, Phys. Rev. B **38**, 5965 (1988); **38**, 9571 (1988).
[15] S. Shin, S. Suga, M. Taniguchi, M. Fujisawa, H. Kanzaki, A. Fujimori, H. Daimon, Y. Ueda, K. Kosuge, and S. Kachi, Phys. Rev. B **41**, 4993 (1990).
[16] M. Abbate, H. Pen, M. T. Czyyk, F. M. F. de Groot, J. C. Fuggle, Y. J. Ma, C. T. Chen, F. Sette, A. Fujimori, Y. Ueda, and K. Kosuge, J. Electron Spectrosc. Relat. Phenom. **62**, 185 (1993).
[17] O. Müller, J. P. Urbach, E. Goering, T. Weber, R. Barth, H. Schuler, M. Klemm, S. Horn, and M. L. denBoer, Phys. Rev. B **56**, 15056 (1997).
[18] R. Zimmermann, R. Claessen, F. Reinert, P. Steiner, and S. Hufner, J. Phys.: Condens. Matter **10**, 5697 (1998).
[19] S.-K. Mo, J. D. Denlinger, H.-D. Kim, J.-H. Park, J. W. Allen, A. Sekiyama, A. Yamasaki, K. Kadono, S. Suga, Y. Saitoh, T. Muro, P. Metcalf, G. Keller, K. Held, V. Eyert, V. I. Anisimov, and D. Vollhardt, Phys. Rev. Lett. **90**, 186403 (2003).
[20] G. Panaccione, M. Altarelli, A. Fondacaro, A. Georges, S. Huotari, P. Lacovig, A. Lichtenstein, P. Metcalf, G. Monaco, F. Offi, L. Paolasini, A. Poteryaev, O. Tjernberg, and M. Sacchi, Phys. Rev. Lett. **97**, 116401 (2006).
[21] M. Taguchi, A. Chainani, N. Kamakura, K. Horiba, Y. Takata, M. Yabashi, K. Tamasaku, Y. Nishino, D. Miwa, T. Ishikawa, S. Shin, E. Ikenaga, T. Yokoya, K. Kobayashi, T. Mochiku, K. Hirata, and K. Motoya, Phys. Rev. B **71**, 155102 (2005).
[22] R. J. O. Mossanek, M. Abbate, and A. Fujimori, Phys. Rev. B **74**, 155127 (2006).
[23] M. A. van Veenendaal and G. A. Sawatzky, Phys. Rev. Lett. **70**, 2459 (1993).
[24] K. Okada and A. Kotani, Phys. Rev. B **52**, 4794 (1995).
[25] R. J. O. Mossanek and M. Abbate, Phys. Rev. B **74**, 125112 (2006).
[26] G. van der Laan, C. Westra, C. Haas, and G. A. Sawatzky, Phys. Rev. B **23**, 4369 (1981).
[27] A. E. Bocquet, T. Mizokawa, K. Morikawa, A. Fujimori, S. R. Barman, K. Maiti, D. D. Sarma, Y. Tokura, and M. Onoda, Phys. Rev. B **53**, 1161 (1996).
[28] S. Klimm, M. Herz, R. Horny, G. Obermeier, M. Klemm, and S. Horn, J. Magn. Magn. Mater. **226**, 216 (2001).
[29] J. J. Yeh and I. Lindau, At. Data Nucl. Data Tables **32**, 1 (1985).
[30] N. Kamakura, M. Taguchi, K. Yamamoto, K. Horiba, A. Chainani, Y. Takata, E. Ikenaga, H. Namatame, M. Taniguchi, M. Awaji, A. Takeuchi, K. Tamasaku, Y. Nishino, D. Miwa, T. Ishikawa, Y. Ueda, K. Kobayashi, and S. Shin, J. Electron Spectrosc. Relat. Phenom. **144**, 841 (2005).